1-1-2012

Microwave-assisted synthesis of flower-like structure ϵ-MnO2 as cathode for lithium ion batteries

Dan Li
University of Wollongong, danli@uow.edu.au

Guodong Du
University of Wollongong, gd616@uow.edu.au

Jieqiang Wang
University of Wollongong, jiew@uow.edu.au

Zaiping Guo
University of Wollongong, zguo@uow.edu.au

Zhixin Chen
University of Wollongong, zchen@uow.edu.au

See next page for additional authors

Article

JOURNAL OF THE CHINESE CHEMICAL SOCIETY

Microwave-assisted Synthesis of Flower-like Structure ε-MnO_2 as Cathode for Lithium Ion Batteries

Dan Li,[a] Guodong Du,[a] Jieqiang Wang,[ab] Zaiping Guo,[ac]* Zhixin Chen[c] and Huakun Liu[a]

[a]*Institute for Superconducting and Electronic Materials, University of Wollongong, NSW 2522, Australia*
[b]*School of Materials Science and Engineering, University of Jinan, Jinan 250022, P. R. China*
[c]*School of Mechanical, Materials & Mechatronics Engineering, University of Wollongong, NSW 2522, Australia*

(Received: Apr. 5, 2012; Accepted: Jun. 4, 2012; Published Online: Jul. 23, 2012; DOI: 10.1002/jccs.201200193)

Nanostructured flower-like ε-MnO_2 and α-MnO_2 nanowires were prepared by the microwave-assisted hydrothermal method at 110 °C and 140 °C. The ε-nanoflowers are about 500 nm in size and are composed of petals about 100 nm in length, while the α-nanowires are 20-30 nm in diameter and about 1 μm in length. The ε-MnO_2 demonstrates higher initial discharge capacity, while the α-MnO_2 shows greater cycling stability in different voltage ranges. Both phases of MnO_2 show better cycling performance in ethylene carbonate (EC)/diethyl carbonate electrolyte (DEC) than in EC/dimethyl carbonate (DMC) electrolyte. The ε-MnO_2 sample delivered a discharge capacity of 116.2 mAh g^{-1} for up to 100 cycles, indicating that it is a promising cathode material for lithium ion batteries.

Keywords: Manganese dioxide; Microwave-assisted hydrothermal; Cathode; Lithium ion batteries.

INTRODUCTION

Nowadays, the rechargeable lithium ion battery is experiencing a huge rise in importance due to the urgent demand for sustainable and renewable power resources.[1] Therefore, intense efforts are very much underway to fabricate promising and environmentally friendly candidate cathode materials to replace the current layered nickel and cobalt oxide materials. Manganese dioxides are some of the most promising positive electrode material due to their intrinsic low toxicity and cost, structural flexibility, high abundance, and chemical stability.[2-4]

Manganese dioxides (MnO_2) exist in many polymorphic forms in which the basic [MnO_6] octahedra are linked in different ways. Examples include α-MnO_2 with [2 × 2] tunnels, rutile structured β-MnO_2 with [1 × 1] tunnels, spinel structured λ-MnO_2 with a three-dimensional network of channels, γ-MnO_2 with an intergrowth of pyrolusite (with [1 × 1] tunnels) and ramsdellite (with [1 × 2] tunnels), and δ-MnO_2 with layered structure. MnO_2 in its diverse structures, showing distinctive chemical and physical properties, is suitable for a wide range of applications, especially as for cathode materials for alkaline batteries[5] and lithium ion batteries.[6-7] Among all these MnO_2 polymorphs, ε-MnO_2 is considered to belong in the same classification as γ-MnO_2, only exhibiting more structural defects (known as microtwinning).[8] Although ε-MnO_2 could be used as a precursor to prepare spinel $LiMn_2O_4$[9] and has recently been reported as supercapacitor electrode,[10-12] there are rare reports of ε-MnO_2 as cathode for lithium intercalation.

Among the facile preparation methods to synthesize nanostructured materials, the hydrothermal method is an efficient way to prepare MnO_2 with various architectures in the absence of any structure-directing agents or templates. In the last few years, the combination of microwave and hydrothermal techniques has been used to prepare inorganic materials with fine nanostructures. In addition, the use of microwaves increases the kinetics by one or two orders of magnitude over the conventional hydrothermal method, so it can reach the same goal in a shorter reaction time or at lower treatment temperatures.[13-14] Materials with three-dimensional (3D) architectures have attracted much attention because of their attractive chemical and physical properties. It has been reported that 3D architecture could produce more active sites or exhibit more attractive electrical, optical, and magnetic properties than 1D and 2D structures.[15]

In the present work, flower-like ε-MnO_2 with 3D hierarchical structure was synthesized via the microwave-assisted hydrothermal method and tested as cathode material

Special Issue for the Electrical Energy Storage and Conversion

* Corresponding author. Tel: (+61) 2 4221 5225; Fax: (+61) 2 4221 5731; E-mail: zguo@uow.edu.au

for lithium ion batteries. As a comparison, α-MnO_2 nanowires were also prepared by the same method by slightly changing the preparation conditions. The morphology and electrochemical properties of both types of MnO_2 were investigated. It was found that the obtained 3D flower-like ε-MnO_2 architecture provides more possibilities to serve as an ideal host material for the insertion and extraction of lithium ions than the α-MnO_2 nanowires due to the unique 3D nanoporous structure of the former material.

EXPERIMENTAL

Synthesis

All chemical reagents in this work were analytical grade and were used as received. ε-MnO_2 nanoflowers: 0.02 mol $MnCO_3$ and 0.02 mol $Fe(NO_3)_3 \cdot 9H_2O$ were dissolved in 200 mL deionized water. 0.04 mol HNO_3 was added to yield a transparent solution. Then, 0.02 mol $(NH_4)_2S_2O_8$ was dispersed in the solution, which was diluted to 300 mL. 20 mL concentrated H_2SO_4 was added, and the solution was diluted to 400 mL. After stirring for 30 min, the solution was sealed in an autoclave and heated at 110 °C for 3 h. α-MnO_2 nanowires: 0.02 mol $MnCO_3$ and 0.0066 mol $Co(NO_3)_2 \cdot 6H_2O$ were dissolved in 200 mL deionized water. 0.04 mol HNO_3 was added to yield a transparent solution. Afterwards, 0.02 mol $(NH_4)_2S_2O_8$ was dispersed in the solution, which was diluted to 300 mL. 20 mL concentrated H_2SO_4 was added, and the solution was diluted to 400 mL. After stirring for 30 min, the solution was sealed in an autoclave and heated at 140 °C for 1 h. The obtained precipitates were collected by centrifuging and washing with deionized water before drying at 80 °C overnight.

Characterization

X-ray diffraction (XRD) patterns were collected using Cu Kα radiation (MMA GBC, Australia). Field emission scanning electron microscope (FESEM) images were collected using a JEOL 7500F microscope. Transmission electron microscope (TEM) investigations were performed using a JEOL 2011F analytical electron microscope (JEOL, Tokyo, Japan) operating at 200 keV. X-ray photoelectron spectroscopy (XPS) experiments were carried out on a VG Scientific ESCALAB 220IXL instrument using aluminum KR X-ray radiation during XPS analysis.

Electrochemical measurements

The electrochemical tests were carried out via CR2032 coin type cells. The working electrodes were prepared by mixing the as-prepared MnO_2, carbon black (Super P, MMM, Belgium), and poly (vinyl difluoride) (PVdF) at a weight ratio of 80:10:10 and were pasted on pure Al foil. The coated electrodes were dried in a vacuum oven at 110 °C for 8 h. Coin cells were assembled in an argon-filled glove box (Mbraun, Unilab, Germany) by stacking a porous polypropylene separator containing liquid electrolyte between the composite electrode and a lithium foil counter electrode. The electrolyte consisted of a solution of 1 M $LiPF_6$ in ethylene carbonate (EC)/dimethyl carbonate (DMC) (1:1, in volume) or ethylene carbonate (EC)/diethyl carbonate (DEC) (1:2, in volume). The charge and discharge measurements were carried out on a Land CT2001 battery test system (Wuhan, China).

RESULTS AND DISCUSSION

It has been reported that pressure and inorganic ion concentration play important roles in controlling the structure and morphology of the final products, involving various types of packing of $[MnO_6]$ octahedra with different edge and corner sharing motifs in different MnO_2 polymorphs, where the ions can stabilize the tunnel structure.[16] In this paper, besides the same cations of NH_4^+ and H^+ which were used as possible stabilizing ions in both α-MnO_2 and ε-MnO_2,[17] Fe^{2+} was also introduced to synthesize ε-MnO_2, as well as Co^{2+} to synthesize α-MnO_2. Highly symmetrical tunnels ([1 × 1] or [2 × 2]) are more stable, but lower pressure is favourable for the less symmetrical structure ([1 × 2]), so the applied temperatures were 110 °C and 140 °C for ε-MnO_2 (an intergrowth of [1 × 1] tunnels and [1 × 2] tunnels) and α-MnO_2 ([2 × 2] tunnels), respectively.

The chemical reaction that took place in the system can be described as follows:

$$MnCO_3 + (NH_4)_2S_2O_8 + H_2O \rightarrow MnO_2 + (NH_4)_2SO_4 + H_2SO_4 + CO_2 \quad (1)$$

The X-ray diffraction patterns are shown in Fig. 1. The reflections can be indexed to tetragonal α-MnO_2 (JCPDS No. 44-0141, Space Group I 4/m) and hexagonal ε-MnO_2 (JCPDS No. 30-0820, Space Group P63/mmc). The peaks are indexed in Fig. 1, and no impurity peaks are found. As the structure of ε-MnO_2 is similar to that of γ-MnO_2, and the absence of any peak at $2\theta = 21^o$ (or $d \approx 4.2$ Å) strongly indicates the highly disordered structure and

confirms the classification of the sample as the originally proposed ε-MnO_2. X-ray photoelectron spectroscopy (XPS) analyses were carried out to confirm the oxidation state of manganese. Fig. 2 shows the Mn 2p spectra. The Mn 2p core level spectra of both samples illustrate the values of the binding energies for Mn 2p3/2 and Mn 2p1/2 (641.9 and 653.4 eV, respectively). The spin-energy separation is 11.5 eV, which is very close to the reported data for Mn $2p_{3/2}$ and Mn $2p_{1/2}$ in MnO_2.[18]

General views of the morphology of the two samples are shown in the FESEM images in Fig. 3(a) and (b). The ε-MnO_2 shows agglomerations of flower-like spheres with diameters ranging from 200 nm to 1 μm, while the α-MnO_2 is composed of thin wires about 1 μm in length. As shown in Fig. 1(a), the entire hierarchical structure of the nanoflower architecture is built up from several dozen nanopetals, which are connected together at the centre to form the 3D flower structure. It has been reported that materials with flower-like spheres have experienced two-stage growth.

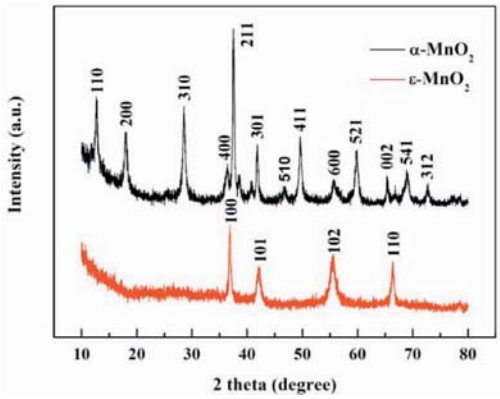

Fig. 1. X-ray diffraction patterns of ε-MnO_2 and α-MnO_2.

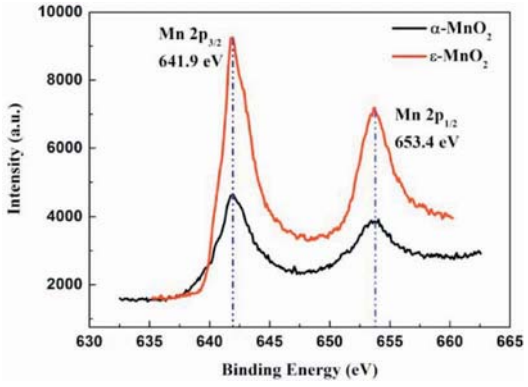

Fig. 2. XPS spectra of the Mn $2p_{3/2}$ and Mn $2p_{1/2}$ regions of ε-MnO_2 and α-MnO_2.

Firstly, the precipitate particles act as nuclei and grow to form the primary particles, which aggregate to become the core of the flower-like structure. Then, the remaining primary particles grow and are aggregated on the core to form the final flower-like structure.[19] The fine structures were investigated by TEM images, as shown in Fig. 3(c)–(f). The TEM images, however, reveal that there is no obvious solid core or shell in the ε-MnO_2 spheres, which are composed of petals about 100 nm in length that are joined together to form a porous structure. The unique structure might be attributed to the fast microwave-assisted hydrothermal treatment, which reduces the reaction time and hinders the growth of the core. The α-MnO_2 wires are about 20-30 nm in diameter and grow along the [100] direction. The inset selected area electron diffraction (SAED) pattern in Fig. 3(f) shows the typical polycrystalline rings.

Fig. 4(a) and (b) shows the discharge and charge profiles of ε and α phase MnO_2 in EC/DMC and EC/DEC electrolyte, respectively. The initial charge/discharge curves are similar in both electrolytes. ε-MnO_2 shows a gradually decrease in voltage with increasing capacity, and the discharge capacity is about 175 mAh g^{-1}, while α-MnO_2 shows a discharge voltage plateau located at 3.0-2.25 V, with a discharge capacity of about 125 mAh g^{-1}. The reac-

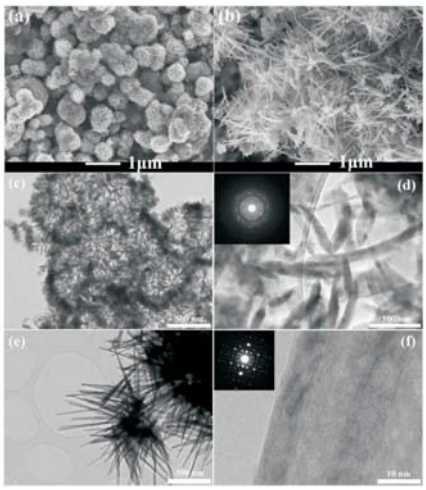

Fig. 3. (a) Low-magnification FESEM image of ε-MnO_2. (b) Low-magnification FESEM image of α-MnO_2. (c) and (d) TEM images of ε-MnO_2, with the inset of (d) showing the SAED pattern of the as-obtained ε-MnO_2. (e) and (f) TEM images of α-MnO_2, with the inset of (f) displaying the SAED pattern of the as-obtained α-MnO_2.

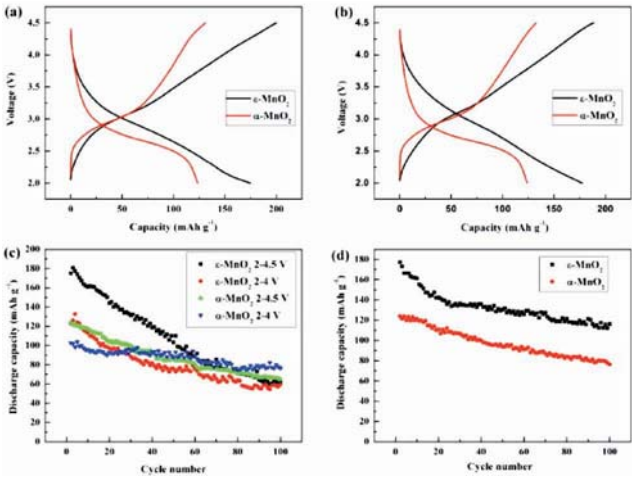

Fig. 4. Electrochemical performance: (a) 2nd cycle charge/discharge curves in EC/DMC electrolyte; (b) 2nd cycle charge/discharge curves in EC/DEC electrolyte; (c) cycling performance in different voltage ranges in EC/DMC electrolyte; (d) cycling performance in EC/DEC electrolyte.

tion can be expressed by the equation:

$$xLi^+ + MnO_2 + xe^- \leftrightarrow Li_xMnO_2 \quad (2)$$

The cycling performance in EC/DMC electrolyte is shown in Fig. 4(c). The discharge capacity of ε-MnO_2 decreases from 175 mAh g^{-1} to 61.4 mAh g^{-1} over 100 cycles in the 2-4.5 V range, and that of α-MnO_2 decreases from 123.6 mAh g^{-1} to 64.6 mAh g^{-1}. In the voltage range of 2-4 V, both samples show greater cycling stability. The capacity of ε-MnO_2 decreases from 122.8 mAh g^{-1} to 59.5 mAh g^{-1}, and that of α-MnO_2 decreases from 102.6 mAh g^{-1} to 76.4 mAh g^{-1}. The cycling performances of both samples are improved in EC/DEC electrolyte, as shown in Fig. 4(d). The ε-MnO_2 delivers a discharge capacity of 116.2 mAh g^{-1} at the 100th cycle, with capacity retention of 65.5% of the capacity of the first cycle, compared with 35.1% in EC/DMC electrolyte, while α-MnO_2 shows capacity retention of 61.5% at the 100th cycle, compared with 52.3% in EC/DMC electrolyte. The phenomenon shows that the EC/DEC electrolyte has better affect on the cycling performance of both ε-MnO_2 spheres and α-MnO_2 than that of EC/DMC electrolyte, indicating that the EC/DEC electrolyte is compatible to MnO_2 for cathode materials. The higher capacity of ε-MnO_2 can be attributed to the 3D flower-like structure, which could provide more active sites for electrode active material and electrolyte, and more conducting pathways for lithium ions and electrons.

CONCLUSIONS

In conclusion, flower-like ε-MnO_2 spheres and α-MnO_2 nanowires have been synthesized by a microwave-assisted hydrothermal method. The structure and morphology of both samples were observed by XRD, FESEM, and TEM. The flower-like ε-MnO_2 spheres about 500 nm in size are composed of petals about 100 nm in length, while the α-nanowires are 20-30 nm in diameter and about 1 μm in length. Benefitting from the 3D architecture, the ε-MnO_2 shows high capacity and delivers a discharge capacity above 116.2 mAh g^{-1} for over 100 cycles in EC/DEC electrolyte.

ACKNOWLEDGEMENTS

This work was supported by the Australian Research Council through a Discovery Project (DP1094261) and the Key Subject (Laboratory) Research Foundation of Shandong Province in P. R. China. The authors also would like to thank Dr. Tania Silver in the University of Wollongong for critical reading.

REFERENCES

1. Tarascon, J. M.; Armand, M. *Nature* **2001**, *414*(6861), 359.
2. Komaba, S.; Kumagai, N.; Chiba, S. *Electrochim. Acta* **2000**, *46*(1), 31.
3. Aronson, B. J.; Kinser, A. K.; Passerini, S.; Smyrl, W. H.; Stein, A. *Chem. Mater.* **1999**, *11*, 949.
4. Nakayama, M.; Kanaya, T.; Lee, J.-W.; Popov, B. N. *J. Power Sources* **2008**, *179*(1), 361.
5. Ghaemi, M.; Gholami, A.; Moghaddam, R. B. *Electrochim. Acta* **2008**, *53*(8), 3250.
6. Kim, J.-H.; Ayalasomayajula, T.; Gona, V.; Choi, D. *J. Power Sources* **2008**, *183*(1), 366.
7. Ogata, A.; Komaba, S.; Baddour-Hadjean, R.; Pereira-Ramos, J. P.; Kumagai, N. *Electrochim. Acta* **2008**, *53*(7), 3084.
8. Watanabe, T.; Zhou, H.; Honma, I. *J. Electrochem. Soc.* **2005**, *152*(8), A1568.
9. Kobayashi, S.; Usui, T.; Ikuta, H.; Uchimoto, Y.; Wakihara, M. *J. Am. Ceram. Soc.* **2004**, *87*(6), 1002.
10. Xiao, W.; Xia, H.; Fuh, J.-Y.-H.; Lu, L. *J. Electrochem. Soc.* **2009**, *156*(7), A627.
11. Yu, P.; Zhang, X.; Chen, Y.; Ma, Y. *Mater. Lett.* **2010**, *64*(1), 61.
12. Roberts, A. J.; Slade, R. C. T. *J. Mater. Chem.* **2010**, *20*(16),

3221.

13. Hu, X.; Yu, J. C.; Gong, J.; Li, Q.; Li, G. *Adv. Mater.* **2007**, *19*(17), 2324.
14. Xu, L.; Ding, Y.-S.; Chen, C.-H.; Zhao, L.; Rimkus, C.; Joesten, R.; Suib, S. L. *Chem. Mater.* **2007**, *20*(1), 308.
15. Ding, Y. S.; Shen, X. F.; Gomez, S.; Luo, H.; Aindow, M.; Suib, S. L. *Adv. Funct. Mater.* **2006**, *16*(4), 549.
16. Shen, Y.-F.; Suib, S. L.; O'Young, C.-L. *J. Am. Chem. Soc.* **1994**, *116*(24), 11020.
17. Wang, X.; Li, Y. *Chem-Eur. J.* **2003**, *9*(1), 300.
18. Xiong, Y.; Xie, Y.; Li, Z.; Wu, C. *ChemInform* **2003**, *34*(25), 1645.
19. Zhong, L. S.; Hu, J. S.; Liang, H. P.; Cao, A. M.; Song, W. G.; Wan, L. J. *Adv. Mater.* **2006**, *18*(18), 2426.

